New 3-(2′-Benzimidazolyl)imidazo[1,2-*a*]pyridinium Mesomeric Betaines. Synthesis and Structure

José M. Minguez,† Teresa Gandásegui,† Juan J. Vaquero,† Julio Alvarez-Builla,*,†
José L. García-Navio,† Federico Gago,‡ Angel R. Ortiz,‡ Pilar Gómez-Sal,§,⊥
Rosario Torres,⊥ and María-Melia Rodrigo∥

Departamento de Química Orgánica, Departamento de Farmacología, Departamento de Química Inorgánica, Departamento de Química Física, and Unidad Central de Servicios Analíticos (UCSA), Unidad de Rayos-X, Universidad de Alcalá, 28871 Alcala de Henares, Madrid, Spain

Received February 22, 1993•

Reaction of *N*-[(2′-benzimidazolyl)methyl]pyridinium salts **2** with isothiocyanates results in a series of 3-(2′-benzimidazolyl)imidazo[1,2-*a*]pyridinium 2-thiolate derivatives **3** classified as conjugated mesomeric betaines. S-Methylation followed by deprotonation easily converts **3** into a new family of conjugated betaines **5**. Semiempirical molecular orbital calculations provide complementary information to the X-ray analysis and experimental dipole moments of both betaines.

Azinium azolate and azolium azolate inner salts **1** have been the subject of investigation mainly because their unusually high dipole moments influence their chemistry and properties.[1,2] In the course of studying the chemistry of some azinium *N*-ylides, we found a facile entry into unknown *N*-ylides **2** that are stabilized by a heteroaromatic moiety.[3] Owing to their structure, we envisaged that these *N*-ylides could be converted into new heterocyclic betaines by dipolar cycloaddition with heterocumulenes. Here we describe the synthesis of two new families of conjugated betaines and discuss their structural features on the basis of theoretical calculations, experimental dipole moments, and X-ray structure determinations.

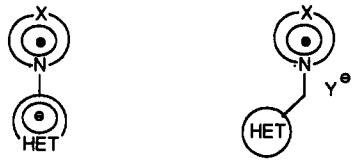

1 **2**

HET = Heteroaromatic
X = CH, N

Results and Discussion

Synthesis. In an earlier paper devoted to the synthesis of *N*-ylides, we found that the reaction of the *N*-(benzimidazolylmethyl)pyridinium salt **2a** with phenyl isothiocyanate resulted in the formation of a mixture of compounds, the betaine **3a** and the *N*-ylide **6** being the major components of the mixture (eq 1). The structures of **3a** and **6** were clearly established on the basis of their analytical and spectroscopic data and some chemical transformations.[4]

Scheme I

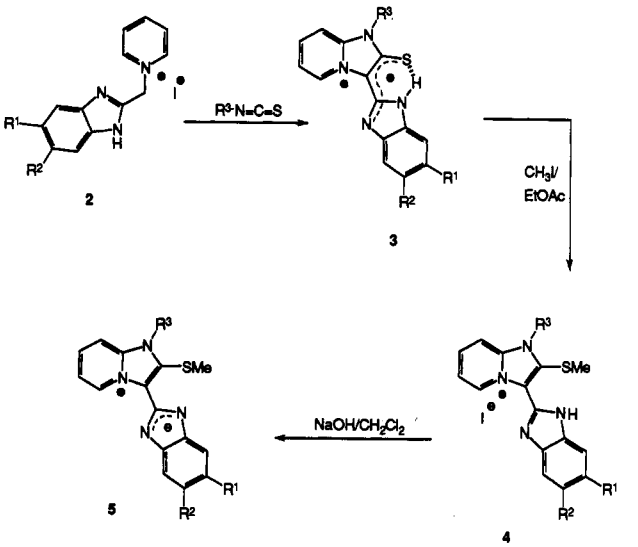

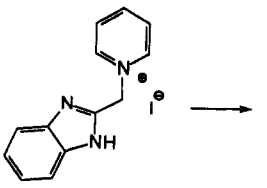

2a

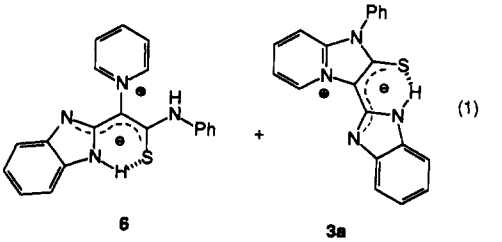

6 **3a** (1)

† Departamento de Química Orgánica.
‡ Departamento de Farmacología.
§ Departamento de Química Inorgánica.
⊥ Unidad Central de Servicios Analíticos (UCSA), Unidad de Rayos X.
∥ Departamento de Química Física.
• Abstract published in *Advance ACS Abstracts*, September 1, 1993.

(1) Alcalde, E.; Dinares, I.; Fayet, J. P.; Vertut, M. C.; Elguero, J. *J. Chem Soc., Chem Commun.* **1986**, 734 and references cited therein.
(2) For a review see" Ollis, W. D.; Stanforth, S. S.; Ramsden, C. A. *Tetrahedron* **1985**, *41*, 2239.
(3) (a) Alvarez-Builla, J.; Sanchez-Trillo, F.; Quintanilla, G. *J. Chem. Soc., Perkin Trans. 1* **1984**, 2693. (b) Cuadro, A.; Alvarez-Builla, J.; Vaquero, J. J. *Heterocycles* **1988**, *27*, 1877. (c) Cuadro, A.; Alvarez-Builla, J.; Vaquero, J. J. *Heterocycles* **1989**, 29, 57.

0022-3263/93/1958-6030$04.00/0

Table I. Physical Data of Betaines 3 and 5 and Salts 4

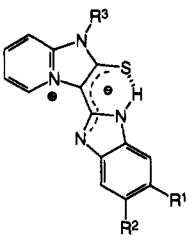

3

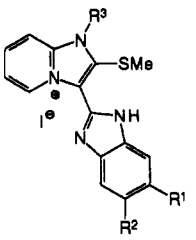

4

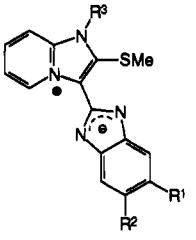

5

compd	R^1	R^2	R^3	reactn time (h)	yield[a] (%)	mp (°C)	crystal habit (solvent)
3a	H	H	C_6H_5	10	47	317–318	yellow needles (CH_2Cl_2–EtOH)
3b	H	H	CH_3	70	21	262–264	brown needles (CH_2Cl_2–EtOH)
3c	H	H	4-ClC_6H_4	24	28	306–308	yellow needles (CH_2Cl_2–EtOH)
3d	Cl	H	C_6H_5	12	31	285–287	yellow needles (CH_2Cl_2–EtOH)
3e	Cl	H	CH_3	72	35	272–273	brown needles (CH_2Cl_2–EtOH)
3f	Cl	H	4-ClC_6H_4	20	27	314–316	yellow needles (CH_2Cl_2–EtOH)
3g	CH_3	CH_3	C_6H_5	22	48	>360	orange needles (CH_2Cl_2–EtOH)
4a	H	H	C_6H_5	36	67	259–261	white plates (EtOH)
4b	H	H	CH_3	48	86	240–241	white plates (EtOH–Et_2O)
4c	H	H	4-ClC_6H_4	40	84	275–277	white plates (EtOH)
4d	Cl	H	C_6H_5	38	71	262–264	white plates (EtOH)
4e	Cl	H	CH_3	60	53	208–210	brown plates (EtOH–Et_2O)
4f	Cl	H	4-ClC_6H_4	48	70	299–300	white plates (EtOH–Et_2O)
4g	CH_3	CH_3	C_6H_5	48	81	310–312	white plates (EtOH)
5a	H	H	C_6H_5	2	73	220–221	yellow powder (CH_2Cl_2–AcOEt)
5b	H	H	CH_3	8	43	219–221	white powder (CH_2Cl_2–AcOEt)
5c	H	H	4-ClC_6H_4	4	49	229–231	yellow powder (CH_2Cl_2–AcOEt)
5d	Cl	H	C_6H_5	3	62	213–215	white powder (CH_2Cl_2–AcOEt)
5e	Cl	H	CH_3	10	49	201–203	brown powder (CH_2Cl_2–AcOEt)
5f	Cl	H	4-ClC_6H_4	12	69	244–246	yellow powder (CH_2Cl_2–AcOEt)
5g	CH_3	CH_3	C_6H_5	8	75	192–194	yellow powder (CH_2Cl_2–AcOEt)

[a] Compounds **3a**, **3c**, **3d**, **3f**, and **3g** were obtained by method A. Compounds **3b** and **3e** were obtained by method B.

This result stimulated us to investigate the appropriate conditions for the efficient preparation of several examples of this class of compounds **3**. Although attempts to obtain the desired betaines by reaction of salts **2** with isocyanate derivatives failed under different conditions, the reaction of *N*-[(2′-benzimidazolyl)methyl]pyridinium salts **2** with isothiocyanates in a two-phase system resulted in the formation of betaines **3a–g** as the main reaction product (Scheme I). These compounds, classified as conjugated heterocyclic mesomeric betaines, isoconjugate with the odd nonalternant hydrocarbon trianion according to Ollis and coworkers,[2] are all stable in the air and exhibit intensely fluorescent colors.

S-Methylation of **3a–g** followed by deprotonation of the corresponding salts **4a-g** afforded a new family of betaines **5a–g** also classified as conjugated and isoconjugate with the even nonalternant hydrocarbon dianion.[2] The physical data of all new compounds described in this work are shown in Table I (for spectroscopic data see Tables II–V in the supplementary material).

Spectroscopic Methods. The IR spectra of the compounds **3** and **4** showed absorptions in the range of 3250–3100 cm^{-1} (ν_{NH}) while these bands were absent for **5**. ^1H NMR data for betaines **3** and salts **4** also provided strong evidence for the presence of the NH of the benzimidazolyl moiety, with values for the chemical shift of the NH proton in the range of δ = 13.2–11.7 ppm.

^1H NMR betaines proved to be very important for the structural proof of the highly dipolar structure of these betaines. In those cases in which comparison of chemicals shifts is possible (Table VI), the CH resonance of the benzimidazolyl moiety in compounds **3** and **5** is shifted upfield with respect to the salts **4**, indicating a higher electron density on the benzimidazole ring in both betaines and especially in **5**. Thus, the observed chemical shift difference between the betaines **3** and the salts **4** is about 0.2 ppm for H-6′ whereas the difference between betaines **5** and the corresponding salts **4** for the same proton is in the range 0.3–0.5 ppm. Moreover, the chemical shift values of H-8 also reflect a higher electron density on the imidazo[1,2-*a*]pyridinium ring, although in this case the observed chemical shift difference between **3** and **4** (0.7–0.9 ppm) is higher than the difference between **5** and **4** (0.11–0.12 ppm). These data are in agreement with negative charge delocalization, mainly over the benzimidazole ring on betaines **5** and over the imidazo[1,2-*a*]pyridinium ring on betaines **3**.

Table VI. Selected ^1H Spectra Data of Several Betaines 3 and 5 and Their Corresponding Salts 4

compd	H-5	H-8	H-6′
3b	10.48	7.73	
4b	10.07	8.42	
5b	10.52	8.28	
3d	10.38		7.22
4d	10.15		7.43
5d	10.88		6.91
3e	10.42	7.52	7.21
4e	10.01	8.41	7.39
5e	10.41	8.29	7.08
3f	10.38		7.21
4f	10.13		7.40
5f	10.82		6.86

As expected, the chemical shift values of the H-5 proton in **3** (δ = 10.38–10.48 ppm) are shifted upfield with respect to **5** (δ = 10.52–10.88 ppm); however, the shielding of this proton in salts **4** (δ = 10.01–10.15 ppm) is significant. This apparently anomalous chemical shift, in terms of charge density, can be rationalized by the different effect of the

(4) Cuadro, A.; Novella, J. L.; Molina, A.; Alvarez-Builla, J.; Vaquero, J. J. *Tetrahedron* **1990**, *46*, 6603.

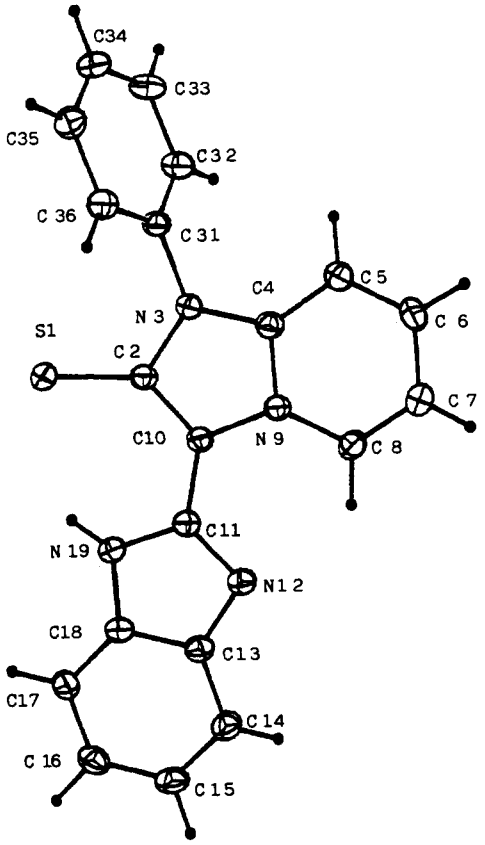

Figure 1. Computer-generated perspective drawing of **3a** with the atom numbering[9] used in the crystal structure analysis.

benzimidazolyl moiety on this proton in betaines **3** and **5** and salts **4**. In this respect, although X-ray data and theoretical methods confirm an almost planar structure for **3a**, **4a**, and **5a**, the hydrogen bond predicted between the H-5 and the nitrogen on the benzimidazole ring (see below, theoretical study) may affect the chemical shift of this proton,[5] especially in compounds **5**. Finally, δC values of carbon atoms (compounds **3a**, **4a**, and **5a**) were in good agreement with previously reported data for benzimidazole and benzimidazolate ions.[6,7]

X-ray Data. The molecular structure of the 3-(2′-benzimidazolyl)-1-phenylimidazo[1,2-*a*]pyridinium 2-thiolate **3a** was determined by X-ray diffraction analysis (a perspective diagram is given in Figure 1, and the unit cell is shown in Figure 2) but attempts to obtain a good single crystal of the betaines **5** failed.[8] Figure 1 shows that the betaine **3a** is virtually planar, the angle between the mean plane of the benzimidazole ring and the mean plane of the imidazo[1,2-*a*]pyridinium ring being 3.6°. The phenyl group is twisted 116° from the plane of the bicyclic system. The X-ray analysis confirmed the intramolecular hydrogen bond in compound **3a** (S1···N19 = 3.130(1) Å and S1···H19 = 2.486(1) Å) and the low contribution of canonical forms with double-bond character for the union bond of both heteroaromatic ring systems (interannular distance C(10)–C(11) = 1.447 Å), proving a low degree of delocalization of negative charge over the benzimidazolyl moiety. Selected bond lengths and angles are shown in Tables VII and VIII, and full atomic coordinates have been deposited with the Cambridge Crystallographic Data Centre (Tables IX–XII).[22]

Table VII. Calculated Bond Distances and Bond Orders for 3a Compared with Data from the X-ray Structure with Esd's in Parentheses

		AM1		PM3	
	X-ray dist (Å)	dist (Å)	bond order	dist (Å)	bond order
S1–C2	1.690(2)	1.588	1.436	1.648	1.695
C2–N3	1.412(3)	1.432	1.010	1.435	1.136
C2–C10	1.382(3)	1.445	1.263	1.426	1.295
C7–H7	0.920(1)	1.100	0.939	1.096	0.962
C8–H8	0.990(2)	1.109	0.907	1.109	9.920
C8–N9	1.377(3)	1.370	1.177	1.387	1.215
C10–N9	1.399(3)	1.405	1.070	1.403	1.177
C10–C11	1.447(4)	1.443	1.034	1.439	1.042
C11–N12	1.326(3)	1.363	1.516	1.361	1.490
C11–N19	1.361(3)	1.410	1.154	1.401	1.248
C31–N3	1.440(3)	1.416	0.943	1.447	0.981
N19–H19	0.851(2)	1.000	0.834	1.001	0.923
S1···N19	3.13	3.03		3.14	
N12···C8	2.96	3.06		2.96	

Table VIII. Calculated Angles for 3a Compared with Data from the X-ray Structure with Esd's in Parentheses

	X-ray	AM1	PM3
S1–C2–N3	123.5(2)	125.68	126.24
S1–C2–C10	131.1(2)	128.98	128.85
S1–H19–N19	132.9(2)	128.76	126.65
C2–N3–C31	126.1(2)	126.36	127.05
C2–C10–C11	128.7(2)	126.55	127.54
C8–H8–N12	127.2(2)	120.77	122.03
C10–C11–N19	120.6(2)	121.09	124.31
C10–C11–N12	125.9(2)	126.03	125.32
C11–N19–H19	124.8(2)	124.70	124.43
N9–C10–C11–N12	3.7(4)	0.11	0.20
C32–C31–N3–C4	62.8(3)	42.50	53.50
C36–C31–N3–C4	−117.1(3)	−138.40	−126.96

Theoretical Study. In order to calculate some relevant molecular properties, a theoretical investigation of these betaines was undertaken by means of the semiempirical molecular orbital program MOPAC.[10] The MNDO,[11] AM1,[12] and PM3[13] Hamiltonians were used for comparison and all $3N-6$ degrees of freedom were optimized. In order to assess the validity of the current parameterization within MOPAC for this class of molecules, we started by comparing the crystal structure of **3a** with the quantum-mechanically, fully-optimized geometries. The MNDO method provided a nonplanar structure (interannular twist angle of 30.68°) with the phenyl ring orthogonal to the imidazo[1,2-*a*]pyridinium ring, which is a poor representation of the experimentally determined geometry. On the other hand, the root-mean-square (rms) displacements for atoms other than hydrogens of the AM1 and PM3

(5) For a similar type of hydrogen bond for pyridinium derivatives see: Spitsin, N. V.; Kochkanyan, R. O. *Khim. Geterotsinkl. Soedin.* **1989**, *5*, 626.

(6) Alcalde, E.; Dinarés, I.; Elguero, J.; Fayet, J.-P.; Verut, M.-C.; Miratvilles, C.; Molins, E. *J. Org. Chem.* **1987**, *52*, 5009.

(7) (a) Alcalde, E.; Dinares, I.; Frigola, J.; Jaime, C.; Fayet, J. P.; Vertut, M. C.; Miravitlles, C.; Molins, E. *J. Org. Chem.* **1991**, *56*, 4223. (b) Alcalde, E.; Perez-Garcia, L.; Miravitlles, C.; Rius, J.; Valenti, E. *J. Org. Chem.* **1992**, *57*, 4829.

(8) The reflections obtained from a very small and low-quality single crystal of **5a** allowed us to obtain a "squeleton structure" without possibility of refinement.

(9) To facilitate comparison of geometries obtained by X-ray and theorehical methods the numbering system used in the X-ray data is the same for the calculated geometries and different from the IUPAC numbering system.

(10) MOPAC and INSIGHT were implemented on a CYBER 910–480 workstation.

(11) Stewart, J. J. P. MOPAC version 6.0; QCPE 455, Quantum Chemistry Program Exchange, Indiana University, Bloomington, IN 47405.

(12) Dewar, M. J. S., Thiel, W. *J. Am. Chem. Soc.* **1977**, *99*, 4899.

(13) Dewar, M. J. S.; Zoebisch, E. G.; Healy, E. F.; Stewart, J. J. P. *J. Am. Chem. Soc.* **1985**, *107*, 3902.

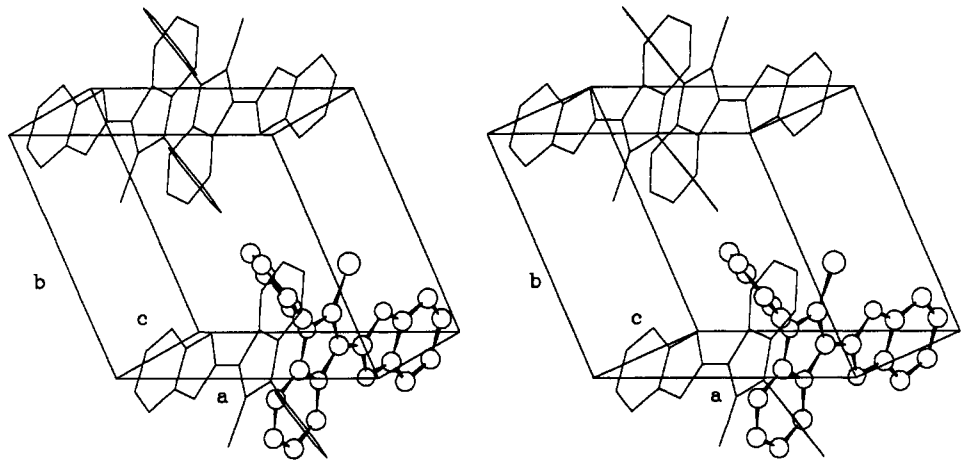

Figure 2. Stereoview of the unit cell packing arrangement of **3a**. The asymmetric unit is shown as the CPK model.

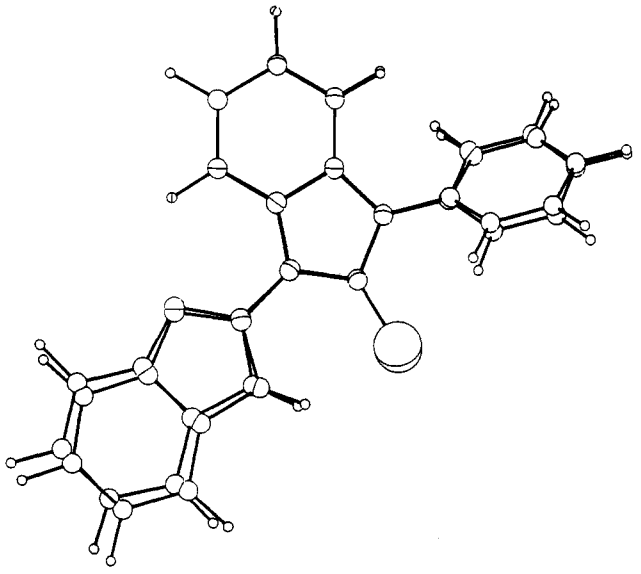

Figure 3. Superimposition of the AM1- and PM3-optimized structures of **3a**.

calculated structures with respect to the X-ray structure were 0.183 and 0.121 Å, respectively. The major difference between these two theoretical structures affects the benzimidazole and imidazo[1,2-*a*]pyridinium rings junction (Figure 3 and Tables VII and VIII) and can be a consequence of the different ability of each method to represent hydrogen-bonding interactions. Partition of the total energy into the different interatomic contributions allowed us to get an estimate of −0.9463 eV (AM1) and −0.7759 eV (PM3) for the hydrogen bond between S1 and H19, and −0.3900 eV (AM1) and −0.5555 (PM3) for that between N12 and H8 (H5 according to the IUPAC numbering system).

In view of the satisfactory results obtained for **3a** with both the AM1 and PM3 Hamiltonians, the salt **4a** and the betaine **5a** were modeled from **3a** with the aid of a molecular modeling program,[14] and their geometries were also fully optimized. Both the Broyden–Fletcher–Goldfarb–Shanno (BFGS) and the Davidon–Fletcher–Powell (DFP) optimization procedures yielded unacceptably large final gradient norms for some molecules and even failed in some cases. On the other hand, the minimization algorithm proposed by Baker[15] for the location of transition states (keyword EF) and a step-size of 0.05 (Å or radians) allowed full geometry optimization to a gradient norm of 0.01 kcal/mol in all cases. Tables XIII and XIV summarize some of the geometrical parameters for the minimum energy conformer of **5a**. For this molecule, the quality of the data available from X-ray diffraction was not good enough for comparison. As was the case for **3a**, the interannular bond has single bond character. As expected, the S1–C2 bond is weaker than in **3a**, and the two benzimidazole ring nitrogens are almost equivalent. Again some minor discrepancies are apparent between the AM1- and PM3-optimized structures which can be readily seen in Figure 4. The more open C2–C10–C11 angle in the PM3-optimized structure is probably a consequence of the larger attraction between N12 and H8 estimated by this method (−2.1309 eV vs −0.5337 eV in AM1) which is also reflected in the smaller N12···C8 distance (*cf.* Table XIII). This results in a rotation of the SCH_3 group toward the benzimidazole nitrogen that appears to be coupled to

Table XIII. Calculated Bond Distances and Bond Orders for 5a

	AM1		PM3	
	dist (Å)	bond order	dist (Å)	bond order
S1–C2	1.669	1.026	1.744	1.005
S1–C37[a]	1.755	0.983	1.793	0.994
C2–C10	1.420	1.446	1.398	1.489
C10–C11	1.429	1.104	1.438	1.056
C11–N12	1.405	1.257	1.396	1.305
C11–N19	1.398	1.278	1.384	1.379
S1···N19	3.22		3.61	
N12···C8	2.95		2.67	

[a] The carbon atom of the methylthio group is numbered as C37.

Table XIV. Calculated Angles for 5a

	AM1	PM3
S1–C2–N3	121.16	118.83
C37–S1–C2[a]	106.21	107.57
S1–C2–C10	131.57	134.43
C2–C10–C11	129.38	134.39
C10–C11–N19	122.25	126.90
C10–C11–N12	122.85	121.21
N9–C10–C11–N12	4.03	1.66
C32–C31–N3–C4	43.08	85.61
C37–S1–C2–N3[a]	121.39	153.59

[a] The carbon atom of the methylthio group is numbered as C37.

(14) Stewart, J. J. P. *J. Comput. Chem.* **1989**, *10*, 221.

(15) INSIGHT-II (version 2.1.0) 1992; Biosym Technologies, 9685 Scarnton Road, San Diego, CA 92121-2777.

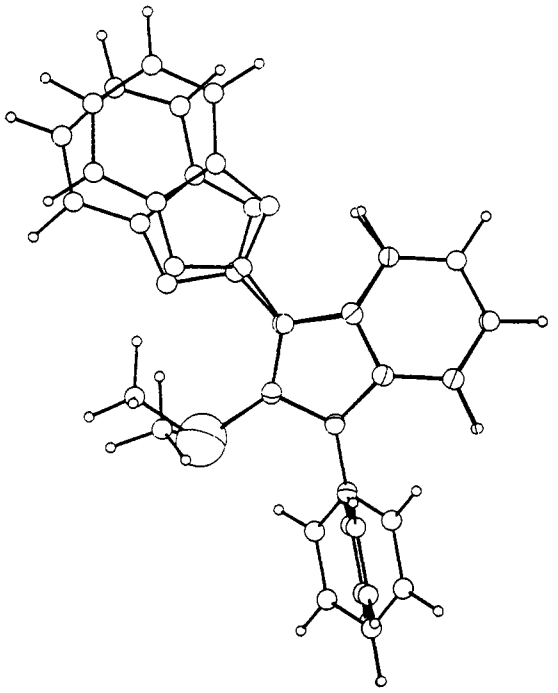

Figure 4. Superimposition of the AM1- and PM3-optimized structures of **5a**.

the rotation of the phenyl ring which thus becomes orthogonal to the plane of the imidazo[1,2-*a*]pyridinium ring. For **4a**, both methods reflect a very low attraction between N12 and H8 (−0.0044 eV in AM1 and −0.0555 eV in PM3).

For **3a**, **4a**, and **5a**, the dependency of the stability of each molecule on the twist angle around the interannular C10–C11 bond was also explored. The torsional space available to the N9–C10–C11–N12 dihedral angle was divided in 15° intervals (plus two additional points at 5° and −5°), and the remaining degrees of freedom of each rotamer were fully optimized as before, using both the AM1 and the PM3 methods. Use of the MNDO Hamiltonian for **3a** revealed that the global minimum described above was very close in energy to the planar structure (Figure 5) found in the crystal and by both the AM1 and PM3 Hamiltonians, but this method was not pursued any further in the study of the rotational barriers. Rotations about the interannular bond in **4a** and **5a** were found to be accompanied by changes in the relative orientation of both the methyl group and the phenyl ring, and different minima were found. For **4a** the lower energy conformer was found to be that in which both heteroaromatic systems are twisted 7°, with the lone pairs on the sulfur, and not the methyl group, pointing in the direction of the NH. In the lower energy conformers of **5a** the methyl group is pointing towards the benzimidazole ring all along the reaction coordinate with the sulfur lone pairs pointing towards the phenyl ring.

As expected, the energy barrier to rotation about the N9–C10–C11–N12 torsional angle is highest for **3a** (Figure 6), partly due to the existence of the two hydrogen bonds reported above which further stabilize the planar structure at 0°, and also due to the steric clash that takes place when H19 approaches H8 as the benzimidazole ring is rotated 180° with respect to the crystal structure. It should be born in mind, however, that the proton could be located on either the N12 or the N18 nitrogen, and therefore the barrier for rotations above +90° or below −90° is somewhat artificial. This is actually reflected in Figure 6, and especially in Figure 6a, since the sides of the curve are shown to be biphasic with an inflection at the point where the benzimidazolyl ring is orthogonal to the imidazo[1,2-*a*]pyridinium ring. In regard to the salt **4a**, a similar pattern emerges (Figure 7) since the proton could be located on the alternative benzimidazolyl nitrogen atom, and the same restrictive interpretation of the height of the barrier applies. This effectively means that one of the nitrogens is actually favored for protonation over the other.

Due to the fact that **5a** presents two equivalent nitrogen atoms on the benzimidazole ring, the resulting curves

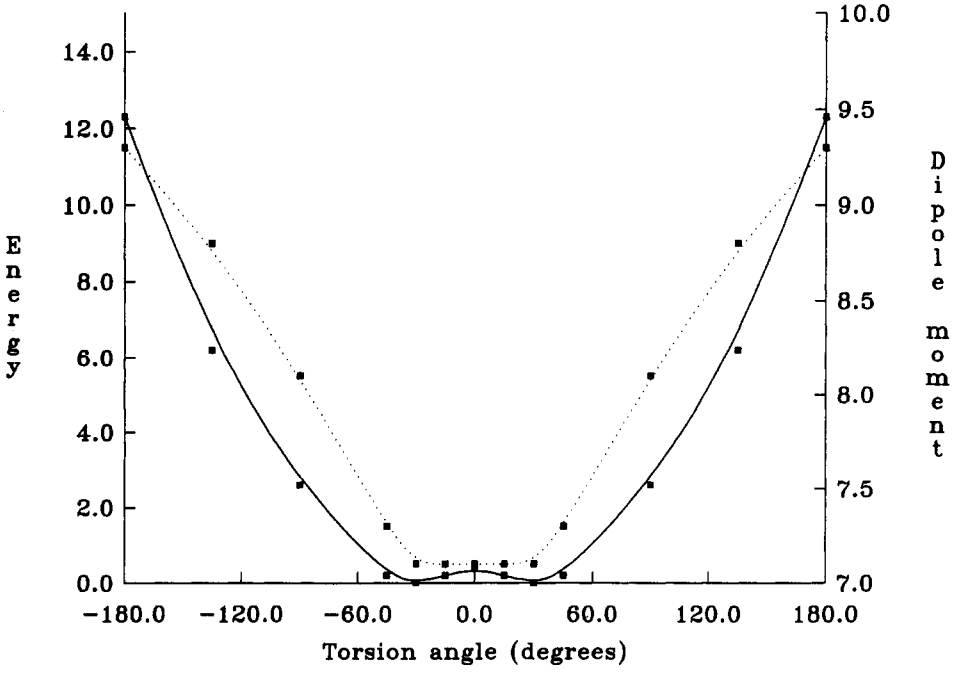

Figure 5. Energy barrier (—, kcal/mol) and variation in dipole moment (···, D) as a function of rotation about the interannular C10–C11 bond in 3a using the MNDO Hamiltonian.

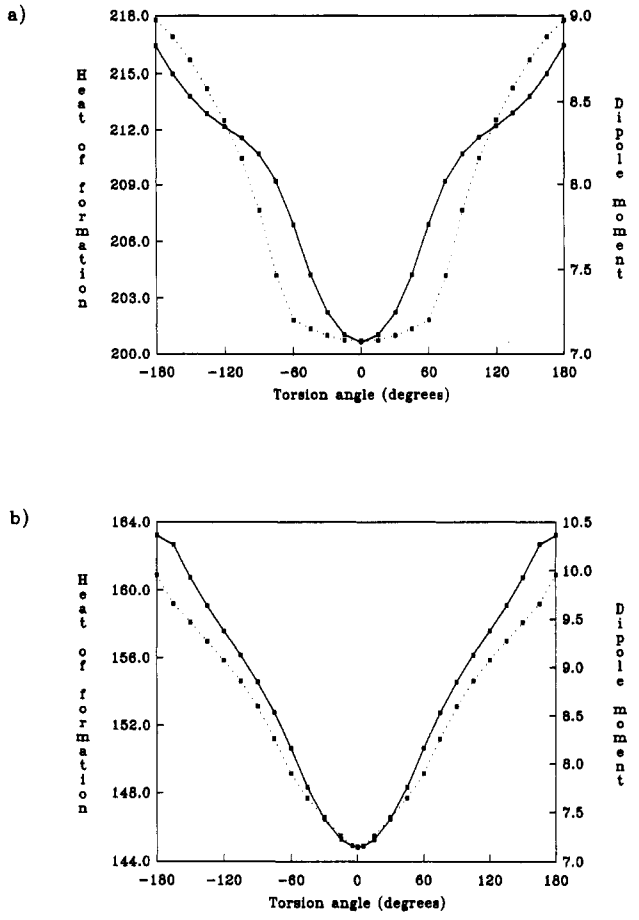

Figure 6. Variation in heat of formation (—, kcal/mol) and dipole moment (···, D) as a function of rotation about the interannular C10–C11 bond in **3a**. (a) AM1, (b) PM3.

Table XV. Experimental *vs* Theoretical Dipole Moments

compd	R^1	R^2	R^3	MNDO	AM1	PM3	exptl
3a	H	H	Ph	7.14	7.07	7.14	6.51
3b	H	H	CH_3	7.00	7.23	7.10	5.29
3d	H	Cl	Ph	8.63	8.20	7.88	7.75
3d	Cl	H	Ph	9.35	8.77	8.41	7.75
3g	CH_3	CH_3	Ph	7.27	6.63	6.71	6.10
5a	H	H	Ph	14.15	12.64	12.13	10.24
5b	H	H	CH_3	13.20	12.15	11.07	10.56
5d	Cl	H	Ph	17.36	14.85	13.78	9.10
5g	CH_3	CH_3	Ph	14.85	12.31	11.77	6.68

(Figure 8) are symmetric with a minimum at 0° and two maxima at ±90°. In the minimum energy structure of this molecule, the attractive interaction between H8 and N12 is greater than in **3a**, reflecting the different charge distribution, and its estimated magnitude again depends on the method used (see above). Therefore, the calculated barrier to rotation is higher when the PM3 Hamiltonian is employed (Figure 8). The geometry of **5a** when the benzimidazole ring is rotated 90° is virtually the same at the AM1 and PM3 levels (rms displacement for all atoms including hydrogens = 0.105 Å) and shows the phenyl ring perpendicular to the imidazo[1,2-*a*]pyridinium ring and the methyl group facing the benzimidazole ring.

Dipole Moments. Theoretical calculations of the betaines **3** and **5** carried out with the three different methods are given in Table XV. An overall comparison with the experimental dipole moments obtained in dioxane and extrapolated to infinite dilution[16] shows that both calculated and experimental methods predict higher dipolar moment values for **5** than for **3**, which is consistent with the higher degree of charge separation in betaines **5**. The comparisons for molecules **5a–b**, **5d**, and **5g** show the similar quality of AM1- and PM3-derived dipole moments and the slightly worse performance of the MNDO method in this respect. The effect of the substituents on the dipole moment is also adequately reproduced except for compound **5d**, for which the calculated trend is opposite to the experimentally observed one. The dipole moments of compounds **3** are all moderately well predicted, the best agreement between the experimental and calculated values being for compound **3d**. For betaines **5**, the calculated values are all clearly overestimated especially for compounds **5d** and **5g**. Similar discrepancies have been reported for related highly dipolar betaines by Alcalde et al. and can be partly accounted for by the perturbing effect of self-association leading to formation of nonpolar dimers in solution,[7] which results in lower measured dipole moments. This is considered to provide an explanation for the results of the present study, and we obtain further support when the dipole moment vectors of **4a** and **5a** are compared (Figure 9). Two major differences are apparent: (i) the larger magnitude of the latter and (ii) the slight change in relative orientation. These effects arise from the different electron density distribution and the increased separation of charges in **5a** relative to **3a** and are translated into slightly different packing arrangement in the solid state. Both **3a** and **5a** give rise to significant intermolecular interactions in the crystals where the favorable orientation of the dipoles is a dominant factor in the electrostatic contribution to the stacking interactions (average intermolecular distance ≈3.5 Å).

For **3d**, two positions are possible for the Cl substituent on the benzimidazole ring (R^1 or R^2). The difference in heat of formation between the two isomers is consistently very small (0.14 [MNDO], 0.06 [AM1], and 0.05 [PM3] kcal/mol) but the lower energy isomer is precisely that with the lower dipole moment, and this value is closer to the experimentally determined, which seems to indicate that this is the tautomer predominantly found in solution.

Experimental Section

General Methods. All melting points were determined on a Buchi SMP-20 apparatus and are uncorrected. IR spectra were obtained as KBr disks on a Perkin-Elmer 1310 spectrophotometer. ^1H NMR and ^{13}C NMR spectra were recorded on a Varian Unity 300 and determined in $(CD_3)_2SO$ or $CDCl_3$, and chemical shifts are expressed in parts per million (δ) relative to internal Me_4Si. Microanalyses were performed on an Heraeus Rapid analyzer for all new compounds within 0.4% error. Mass spectra were obtained on a Hewlett-Packard 5988 A spectrometer. UV spectra were recorded on a Beckman DU-68 spectrometer as methanolic solutions (1.10^{-5} M).

Materials. The *N*-[(2'-benzimidazolyl)methyl]pyridinium salts **2** were prepared as previously reported.[4]

Preparation of Imidazo[1,2-*a*]pyridinium 2-Thiolate Derivatives 3a–g. Method A. To a suspension of the corresponding salt **2** (1 mmol) in 10 mL of dry methylene chloride was added an aqueous solution (50%) of potassium carbonate (10 mL). After the mixture was stirred for a few minutes the isothiocyanate (1.2 mmol) was added, and stirring was continued at room temperature for the time specified in Table I. The organic layer was then separated, and the aqueous phase was extracted with methylene chloride (3 × 20 mL). The combined organic layers were washed with water until neutral, dried with magnesium sulfate, and evaporated under reduced pressure. Chromatography of the solid residue obtained using CH_2Cl_2 or CH_2Cl_2/

(16) Baker, J. *J. Comput. Chem.* **1986**, *7*, 385

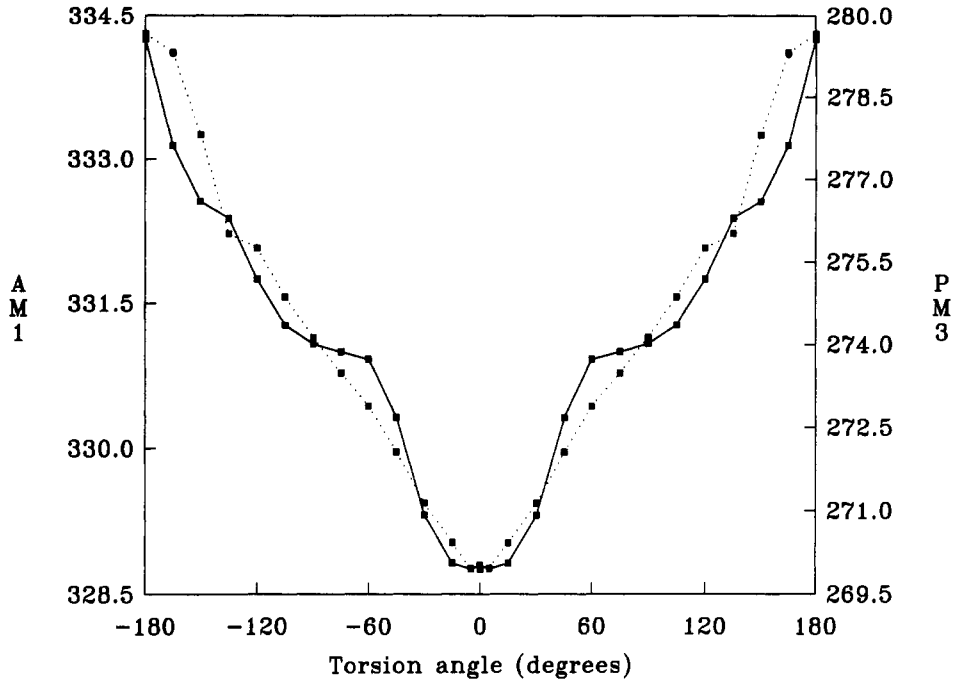

Figure 7. Variation in heat of formation (kcal/mol) as a function of rotation about the interannular C10–C11 bond in 4a using the AM1 (—) or the PM3 (···) Hamiltonians.

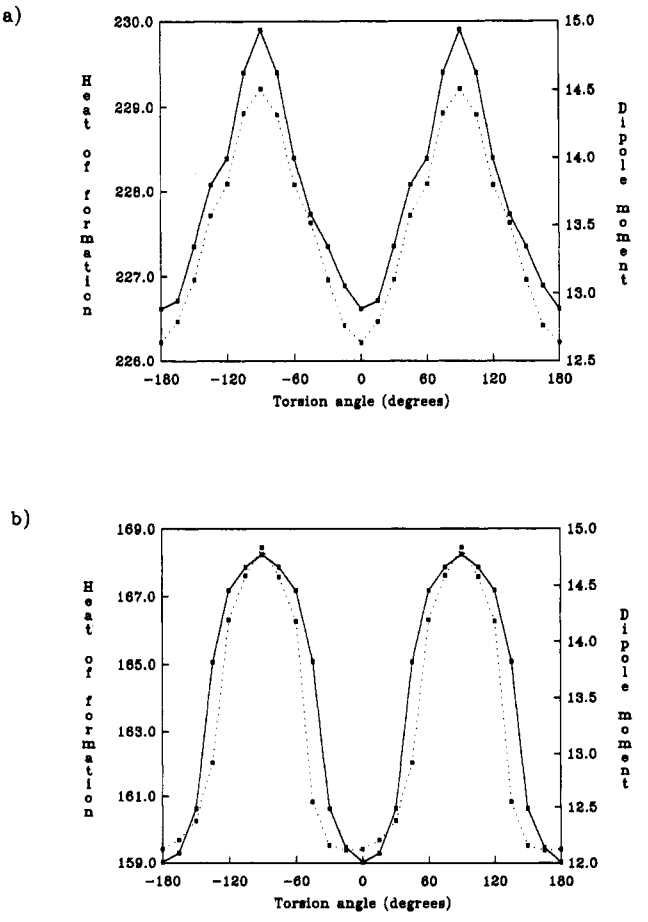

Figure 8. Variation in heat of formation (—, kcal/mol) and dipole moment (···, D) as a function of rotation about the interannular C10–C11 bond in **5a**. (a) AM1, (b) PM3.

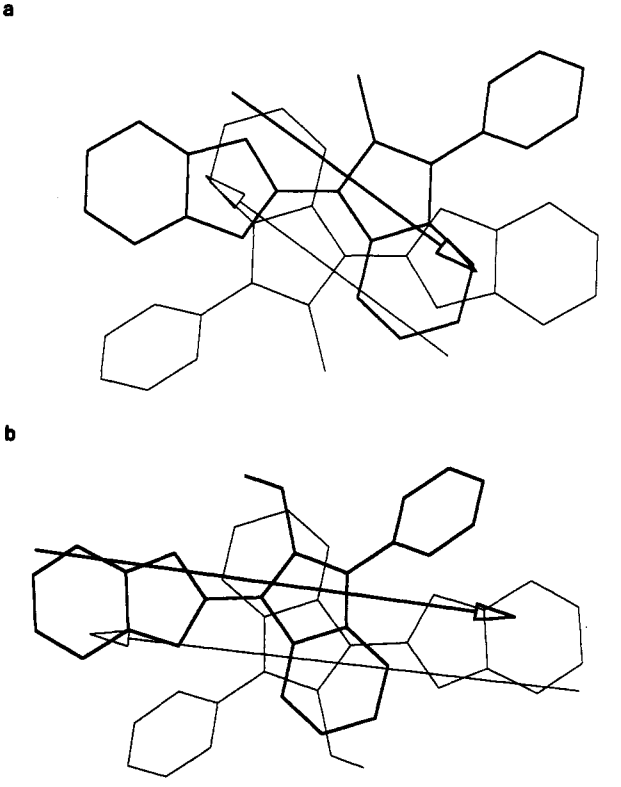

Figure 9. Detailed model of the stacking arrangement found in the crystal packing of **3a** (a) and **5a** (b). The calculated dipole moment vectors are represented by arrows whose midpoints are centered on the geometrical center of each molecule. The geometries have been fully optimized using the AM1 method within MOPAC. The model for **5a** is based on the structure obtained from

acetone (9:1) as eluent followed by recrystallization (see Table I) afforded pure betaines **3a–g**.

Method B. A mixture of the corresponding salt **2** (1 mmol), the isothiocyanate derivative (1.2 mmol), and anhydrous potassium carbonate (4 mmol) in dry acetonitrile (10 mL) was stirred at room temperature for the time specified in Table I. After that time, the reaction mixture was filtered off and the filtrate evaporated under reduced pressure. The residue was dissolved in methylene chloride and the resulting solution washed with

water until neutral, dried with magnesium sulfate, evaporated under reduced pressure, and chromatographed as indicated in method A.

Preparation of 2-(Methylthio)imidazo[1,2-a]pyridinium Salts 4a–g. To a suspension of the corresponding betaine **3a–g** (1 mmol) in ethyl acetate (30 mL) was added methyl iodide (4 mmol), and the mixture was stirred at room temperature for the time specified in Table I. The precipitates formed were collected on a filter and recrystallized to give pure salts **4a–g**.

Preparation of 2-(Methylthio)imidazo[1,2-a]pyridinium 3-(2'-Benzimidazolate) Inner Salts 5a–g. To a suspension of the corresponding salt **4a–g** (0.5 mmol) in methylene chloride (12 mL) was slowly added an aqueous solution of sodium hydroxide (50%, 10 mL) and the mixture stirred at room temperature (for time see Table I). The organic layer was separated, washed with water until neutral, dried over magnesium sulfate, and evaporated under reduced pressure. Recrystallization from the solvents indicated in Table I afforded pure betaines **5a–g**.

Single-Crystal X-ray Structure Determination of Betaine 3a. Crystal data for compound **3a**: Molecular formula: $C_{20}H_{14}N_4S$, M = 342.42, triclinic space group $P\bar{1}$, a = 8.523(1) Å, b = 8.653(4) Å, c = 12.305(3) Å, α = 90.78(1)°, β = 104.26(1)°, γ = 113.51(1)°, U = 800.1(9) Å^3 (by least-squares refinement on diffractometer, angles for 25 automatically centred reflections), λ = 0.7106 Å, Z = 2, D_c = 1.42 g cm^{-3}. Yellow, 0.20 × 0.25 × 0.15 mm^3, μ(Mo Kα) = 2.02, cm^{-1} $F(000)$ = 356. All crystallographic measurements were made in a Enraf-Nonius CAD4 diffractometer, ω/θ mode with ω scan width = 2.40 + 1.05 tan θ,ω scan speed 1.0–8.2 deg min^{-1}, graphite-monochromated Mo Kα radiation; number of reflections measured 3471 [$2.0 \le \theta \le 27°$, $-10 \le h \le 10, -11 \le k \le 11, -15 \le l \le 0$]; 1839 observed reflections with $I > 2\sigma(I)$, two standard reflections were measured every 120 min, and no variation was detected. The structure was solved by direct methods using Multan,[17] Dirdif[18] and SPD Structure Determination Package, Enraf-Nonius Programms.[19] Full-matrix least squares refinement with all non-H atoms anisotropic; all the H-atoms were experimentally determined. Final R and R_w values are 0.039 and 0.044 with

$$R_w = \left[\frac{\sum_w ||F_o| - |F_c||^2}{\sum w|F_o|^2}\right]^{1/2} \qquad w = 4F_o^2/[\sigma|F_o|^2]^2$$

Highest peak in final DF map is 0.18 e Å^{-3}. Source of scattering factors data are given in ref 20.

Dipole Moments. Dielectric constants of solutions of the substances in 1,4-dioxane were measured at 25 °C with the Dipolmeter DM 01 (Wissenschaftlich-Technische Werkstätten) at a fixed frequency of 2.0 MHz. The DFL1 cell was calibrated at 25 °C with compounds of known dielectric constant (i.e., benzene, carbon tetrachloride, and cyclohexane). Increments of the refractive indices of the solutions with respect to the solvent were determined at 25 °C in a Brice-Phoenix 2000-V differential refractometer. Values of the dipole moment were calculated from the equation of Guggenheim and Smith[17]

$$\mu^2 = (27kTM)(4\pi\rho N)^{-1}(\epsilon_1 + 2)^{-2}[(d\epsilon/d\omega) - 2n_1(dn/d\omega)]$$

where k is the Boltzmann constant, T is the absolute temperature, M is the molecular weight of the solute, ρ is the density of the solvent, N is Avogadro's number, and ω is the weight fraction of the solute. The symbols ϵ and n represent, respectively, the dielectric constant and index of refraction of the solutions; the same symbols with the subscript 1 represent the same quantities for the solvent. Values of $d\epsilon/d\omega$ and $dn/d\omega$ were obtained as the slope from plots of the increments of the dielectric constant ($\Delta\epsilon = \epsilon - \epsilon_1$) and the index of refraction ($\Delta n = n - n_1$) against ω, in the vicinity of $\omega \to 0$.

Acknowledgment. We express our thanks to Prof. J. Elguero for helpful discussions. We gratefully acknowledge the University of Alcalá award (J.M.M.) and financial support from Comisión Interministerial de Ciencia y Tecnologia (CYCIT) through the project PB90-0284.

Supplementary Material Available: Characterization data for compounds 3–5 (4 pages). This material is contained in libraries on microfiche, inmediately follows this article in the microfilm version of the journal, and can be ordered from the ACS; see any current masthead page for ordering information.

(17) (a) Guggenheim, E. A. *Trans. Faraday Soc.*, **1949**, *45*, 714; (b) *Ibid.* **1951**, *47*, 573. (c) Smith, J. W. *Trans. Faraday Soc.* **1950**, *46*, 394.

(18) Main, P.; Fiske, S. E.; Hull, S. L.; Lessinger, L.; Germain, G.; Declerq, J. P.; Woolfson, M.M. *MULTAN 80 Program*, University of York (England) and University of Louvain (Belgium), 1980.

(19) Beurkens, P. T.; Bosman, W. P.; Doesburg, H. M.; Could, R. O.; Van der Hark, E. M.;Prick, P. A. J.; Noordik, J. H.; Beurkens, G.; Parthasarathi, V. *DIRDIF Program*, Crystallography Laboratory, Toernooiveld, Netherlands, 1981.

(20) *Structure Determination Package*, B. A. Frenz and Associates, Inc., College Station (Texas 77840) and Enraf-Nonius, Delft (Holland).

(21) International Tables for X-ray Crystallography; Kynoch; Birminghan, England, 1974; Vol. 4.

(22) The coordinates can be obtained, on request, from the Director, Cambridge Crystallographic Data Centre, 12 Union Road, Cambridge, CB2 1EZ, UK.